A Hierarchical Approach for Banknote Image Processing Using Homogeneity and FFD Model

Ye Jin, Ling Song, Xianglong Tang, and Ming Du

Abstract—**This letter presents a novel banknote image processing system that includes banknote recognition, general attrition evaluation, and feature identification, in which the phenomenon of banknote deterioration is discussed in detail for the first time. To compare the sensed image with its reference, a banknote image registration algorithm based on the free-form deformations model (FFD) is proposed, in which a homogeneity-based banknote deterioration energy (BDE) is used as the cost function. The proposed algorithms lead to a high capacity for low-quality banknote processing and greatly decrease the false reject rate.**

Index Terms—**Banknote processing, free-form deformations, homogeneity.**

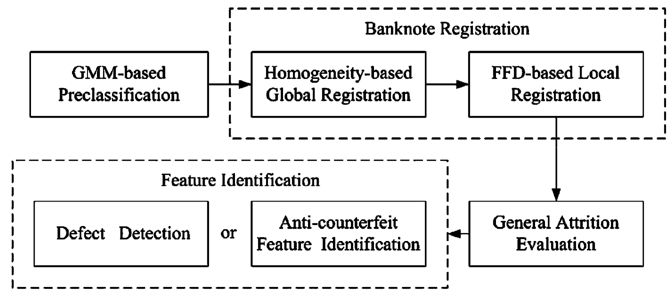

Fig. 1. Banknote image processing diagram.

I. Introduction

THERE is a growing need for automatic banknote processing apparatus in banks and financial institutes. This issue has been a concern since the 1990s last century, including banknote recognition [1], [2], banknote defect detection [3], banknote validation [4], and acoustic signal-based banknote fatigue evaluation [5]. The experimental results illustrate the effectiveness of these methods. As banknotes inevitably deteriorate during the whole circulation, maintaining a high robustness against banknote deterioration is of vital importance for any banknote processing algorithm. However, this issue has not been thoroughly investigated in previous banknote processing methods.

In this letter, we propose a hierarchical approach to banknote processing in which the phenomenon of banknote deterioration is described by a homogeneity-based banknote deterioration energy (BDE). In our banknote processing system, one banknote is orderly sampled by several high-speed contact image sensors in different bands. Each sensed images has a size of 583×68 and a spatial resolution of 0.33×1.4 mm, and it is processed by a special DSP. In one banknote image processing module, as shown in Fig. 1, each sensed image is first pre-classified by a supervised Gaussian mixture model (GMM), and an FFD-based banknote image registration algorithm is then proposed to map the sensed image to the corresponding reference image, in which BDE is used as the cost function. After registration, anti-counterfeit features or local defects can easily be identified.

In Section II, the phenomenon of banknote deterioration and the BDE are discussed in detail. Section III introduces the hierarchical approach for banknote processing. The experimental results are shown in Section IV.

Manuscript received November 8, 2007; revised January 10, 2008. The associate editor coordinating the review of this manuscript and approving it for publication was Dr. Konstantinos N. Plataniotis.

Y. Jin, L. Song, and X. L. Tang are with the Harbin Institute of Technology, Harbin 150001, China (e-mail: jinlailai@gmail.com).

D. Ming is with the Harbin Billsorter Ltd., Harbin 150086, China.

Digital Object Identifier 10.1109/LSP.2008.921470

II. Banknote Deterioration Analysis Using BDE

Banknote deterioration can be viewed as a joint effect of general attrition and local defect. General attrition is regarded as a stabilized and homogeneous color mixture procedure between the banknote and the dusts in circulation. The colors of the dusts are assumed to obey the normal distribution. Conversely, local defect is regarded as an unpredictable influence which can be characterized by an independent random variable.

A. Homogeneity of Banknote Image

Homogeneity is a composition of standard deviation and discontinuity of intensities, which is largely related to the local information extracted from an image and reflects how uniform a region is [6]. Therefore, it is a useful feature for banknote processing: general attrition and local defect have opposite influence on banknote homogeneity. In normal circulation, a banknote gradually turns dark and blurry due to the effect of general attrition, and as a result, the homogeneity value is increased irreversibly. However, when a local defect occurs, a distinct decrease in homogeneity usually appears at the edge of the defect area.

For one sensed image I, we denote the intensity on point $z = (x, y)$ as I_z, and the $D \times D$ rectangle window centering on z as $\Omega(z)$. In our system, we set $D = 5$. Within $\Omega(z)$, the standard deviation on z is calculated as

$$v_z = \sqrt{\frac{1}{D^2} \sum_{p \in \Omega(z)} (I_p - u_p)^2} \tag{1}$$

where u_p is the sliding average of intensity at point p calculated as

$$u_p = \frac{1}{D^2} \sum_{q \in \Omega(p)} I_q. \tag{2}$$

We employ the Sobel operator to calculate the discontinuity and use the magnitude of the gradient on as the measurement

$$e_z = \sqrt{G_h^2 + G_v^2} \tag{3}$$

where G_h and G_v are the components of the gradient in the horizontal and vertical directions, respectively. To compare the homogeneity between different images, we represent the inhomogeneity value of z as

$$h_z = \sqrt{(v_z)^2 + (e_z)^2}. \tag{4}$$

We define the truncated-inhomogeneity-value TIH of z as

$$H(I_z) = \begin{cases} h_{\min}, & h_z < h_{\min} \\ h_z, & h_{\min} \leq h_z < h_{\max} \\ h_{\max}, & h_z \geq h_{\max} \end{cases} \tag{5}$$

where $h_{\min}$ and $h_{\max}$ are the truncating thresholds, which are used to control the potential influence caused by the noise and local defect separately. The truncating thresholds are mainly relative to the common features of banknote deterioration instead of the banknote design. We called them design-independent parameters. In our system, $h_{\min} = 4$ and $h_{\max} = 120$.

B. Banknote Deterioration Energy

For each type of the banknote, we can select an undeformed image sampled from an uncirculated banknote as the reference image. Let us denote a reference image as T. For each point z on T, the squared-color-shift (SCS) of z is defined as

$$\mathbb{Z}(z, z') = k(T_z - I_{z'})^2 \tag{6}$$

where $I_{z'}$ is the corresponding pixel of T_z, and k is the difficulty coefficient reflecting the difficulty of the color shift from T_z to $I_{z'}$. The value of k is calculated as

$$k = \begin{cases} k_1, & (\mu_w - \varepsilon_w) \leq I_{z'} \leq T_z \\ k_2, & T_z \leq I_{z'} \leq (\mu_w + \varepsilon_w) \\ k_3, & \text{else} \end{cases} \tag{7}$$

where μ_w is the expectation of the dust color (intensity), and $\varepsilon_w > 0$ is the corresponding tolerance. They are also design-independent and can be set as below.

Each type of banknote can be classified into five grades, namely, uncirculated, ATM satisfied, recyclable, unrecyclable, and poor. We predefine the general-attrition-rate (GAR) of those grades as $\rho = 0,10,30,50$, and 80, respectively. In the training of the samples, the subregion without printing ink (such as the watermark area) can be treated as a blank area. Let $I_{\text{blank}}(\rho)$ denote the average intensity of the blank area according to a certain ρ; the dust color can be defined as $\mu_w = \lim_{\rho \to 100} I_{\text{blank}}(\rho)$. We can first obtain the expectation of $I_{\text{blank}}(\rho)$ of each grade and then yield μ_w by interpolation. In our system $\mu_w = 128$ and $\varepsilon_w = 10$.

In (7), the first condition $(\mu_w - \varepsilon_w) \leq I_{z'} \leq T_z$ means that the color shifts from a light color to μ_w, in which the colors shift easily and quickly. The second condition $T_z \leq I_{z'} \leq (\mu_w + \varepsilon_w)$ means that the color shifts from a dark color to μ_w, in which the colors shifts slowly because of the stability of the printing ink. The other conditions usually mean mismatch or local defect. Therefore, we set the difficulty coefficients as $k_1 = 1$, $k_2 = 2$, and $k_3 = 5$.

The TIH decrease from T_z to $I_{z'}$ can be written as $HD(z, z') = H(T_z) - H(I_{z'})$. If $HD(z) < \varepsilon_h$ for some small negative value ε_h, it means mismatch or local defect. Usually, we set $\varepsilon_h = -h_{\min}$ and define the squared-homogeneity-difference (SHD) of z as

$$\mathbb{R}(z, z') = \begin{cases} (h_{\max} - h_{\min})^2, & HD(z, z') \leq \varepsilon_h \\ (HD(z, z'))^2, & \text{else.} \end{cases} \tag{8}$$

SCS is sensitive to banknote deterioration, but it is also susceptible to noise. In contrast, SHD has a relatively low sensitivity to banknote deterioration but maintains a high stability to noise. To construct a more robust deterioration feature, we define BDE from z to z' as the weighted sum of SCS and SHD, as follows:

$$\mathbb{Q}(z, z') = \mathbb{R}(z, z') + \alpha \mathbb{Z}(z, z') \tag{9}$$

where α is the weighting parameter, which is also design-independent and usually ranges from 0.25 to 4.

III. Banknote Image Processing System

A. Pre-Classification of Banknote Using Supervised GMM

Similar to [2], the sensed banknote is segmented into $K \times L$ overlapped subregions $\Gamma_{k,l}$, $k = 1, 2, \ldots, K$, $l = 1, 2, \ldots, L$, and the each subregion has the same size $d_x \times d_y$. The original feature vector of the banknote image can be written as $\mathbf{x} = [x_1, x_2, \ldots, x_{K \times L}]$, where $x_{(l-1) \cdot K + k}$ is the intensity mean of the subregion $\Gamma_{k,l}$, as follows:

$$x_{(l-1) \cdot K + k} = \frac{1}{d_x \times d_y} \sum_{z \in \Gamma_{k,l}} I_z. \tag{10}$$

In our system, we set $k = 7$, $L = 31$, and utilize a K_L transform to extract the feature vectors, which usually have the dimensions ranging from 32 to 64. We adopt a supervised GMM for banknote pre-classification. Corresponding to the five grading standards, we predefine the component number of each GMM as 5 and assume these components to have the same mixing probabilities. For each component (grade), the expectation and variance of the feature vectors can easily be yielded through the training of the samples.

B. Deformation Model of Banknote Image

The banknote deformation is interpreted by the FFD formulation, in which the mesh of control points is defined as $C = \{c_{k,l}\}$, where $c_{k,l} = \left(c_{k,l}^x, c_{k,l}^y\right)$ is just the centering points of $\Gamma_{k,l}$. As in [7], denoting the incremental FFD parameters as $\psi = \{\delta C_{k,l}\} = \left\{\left(\delta c_{k,l}^x, \delta c_{k,l}^y\right)\right\}$, the deformed position of each pixel z can defined by a tensor product of cubic B-splines, as follows:

$$\begin{aligned} L(\Psi; z) &= z + \delta L(\Psi; z) \\ &= z + \sum_{m=0}^{3} \sum_{n=0}^{3} B_m(s) B_n(t) \delta C_{i+m, j+n} \end{aligned} \tag{11}$$

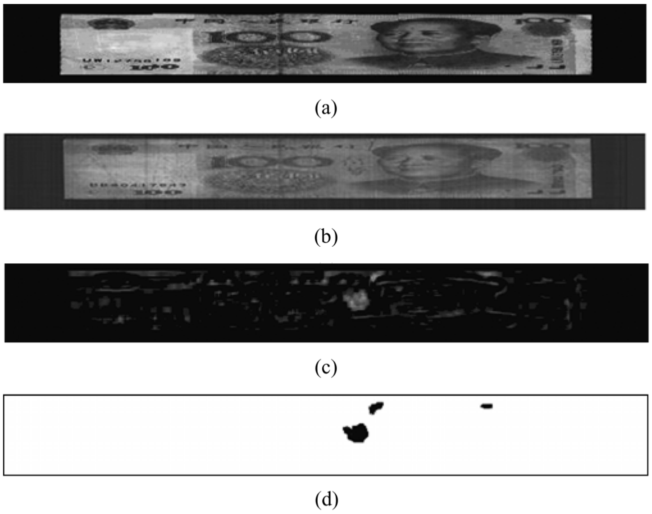

Fig. 2. Banknote image registration and local defect detection. (a) Reference image. (b) Sensed image. (c) Corresponding BDE map. (d) Local defect area.

where $i = [x/d_x] + 1$, $j = [y/d_y] + 1$, $s = x/d_x - [x/d_x]$, $t = y/d_y - [y/d_y]$, and $B_m(s)$ represents the mth basis function of cubic B-spline, as follows:

$$B_0(s) = \frac{(1-s)^3}{6}, \quad B_1(s) = \frac{(3s^3 - 6s^2 + 4)}{6}$$
$$B_2(s) = \frac{(-3s^3 + 3s^2 + 3s + 1)}{6}, \quad B_3(s) = \frac{s^3}{6}. \quad (12)$$

C. Banknote Image Registration Using Binarizated-TIH-Map and BDE-Based Free-Form Deformations

For one subregion $\Gamma_{k,l}$ in T, we can find its corresponding subregion on I, which we denote as Γ'. Assuming that Γ' has the same size with $\Gamma_{k,l}$ and centers on $c_{k,l} + \delta c$, the difference between $\Gamma_{k,l}$ and Γ' can be defined as

$$dif(\Gamma_{k,l}; \delta c) = \frac{\int_{\Gamma_{k,l}} \hat{H}(T_z)\,(T_z - I_{z+\delta c})^2\, dz}{\int_{\Gamma_{k,l}} \hat{H}(T_z) dz} \quad (13)$$

where $\hat{H}(T_z)$ is the binarizated TIH value of T_z calculated as

$$\hat{H}(T_z) = \begin{cases} 0, & h_z < h_{th} \\ 1, & h_z \geq h_{th} \end{cases} \quad (14)$$

where h_z is the homogeneity value of z, and h_{th} is the fixed threshold. When $\hat{H}(T_z) = 1$, z may be considered as a valid point for the global registration. In our system, $h_{th} = 40$. By minimizing (13), the deformed position of $c_{k,l}$ is yielded as

$$\delta c_{k,l} = \arg\min_{\delta c} dif(\Gamma_{k,l}, \delta c) \quad (15)$$

where δc is usually limited to 2 mm in the horizontal direction and 1 mm in the vertical direction.

After global registration, the BDE is engaged as the data-driven term to find the optimal transformation. We define the cost function for the nonrigid registration as

$$E(\Psi) = \int_r \mathbb{Q}(z, L(\Psi; z))dz + \\ +\beta \int_r \left(\left\| \frac{\partial \delta L(\Psi; z)}{\partial x} \right\|^2 + \left\| \frac{\partial \delta L(\Psi; z)}{\partial y} \right\|^2 \right) dz. \quad (16)$$

As in [7], we implement a gradient decent approach to minimize the cost function. Assuming the intensity of the pixels is in the range of 0–1, the typical values for β are in the range of 0.1–0.5.

D. Banknote Image Evaluation

The BDE is also a valid feature that can be used to characterize the general attrition degree. In the training of the samples, we can obtain the BDE expectation of each grade, which we denote as $BDE(\rho)$. After interpolation, we can produce the BDE-GAR curve as shown in Fig. 3, by which the general attrition degree of the sensed image can be easily evaluated.

To evaluate the local defect or anti-counterfeit feature, the sensed image is compared with its corresponding reference image as follows: Calculate the BDE value of each pixel using (9) and normalized as

$$\mathbb{Q}'(z) = \begin{cases} 1, & \mathbb{Q}(z) > \lambda_2 \\ 0.5, & \lambda_1 < \mathbb{Q}(z) \leq \lambda_2 \\ 0.1, & \lambda_0 < \mathbb{Q}(z) \leq \lambda_1 \\ 0, & \mathbb{Q}(z) \leq \lambda_0 \end{cases} \quad (17)$$

where the threshold $\lambda_i, i = 0, 1.2$ can be viewed as the filters to extract the desired information. Let us denote the 3×3 window centering on z as $\delta(z)$. If $\sum_{p \in \delta(z)} \mathbb{Q}'(p) > 1$, I_z is recognized as the local defect or anti-counterfeit feature.

In the local defect detection, usually we set $\lambda_0 = BDE(50)$ the average BDE of the unrecyclable grade, λ_1 the average BDE of the local defect pixels that manually located by the bank clerk, and λ_2 is the average BDE of the seriously defective pixels that must be detected. A sample of local defect detection is show in Fig. 2. We can find that the graffiti on the complicated background can also be detected.

In anti-counterfeit feature detection, λ_i should be set according to the position and the characteristics of the feature that we want to validate. An example of anti-counterfeit feature detection is shown in Fig. 4. On the genuine banknotes [see Fig. 4(a)], the ornamental patterns around the watermark and Gandhi's portrait are invisible under the special infrared, but on the counterfeit banknotes [see Fig. 4(b)], the ornamental patterns still exist. To detect those phenomena, we locate the relative point manually according to the desired feature and set $\lambda_i = 0$ for the other irrelative area. For each relative point z, we can obtain its BDE expectations in the genuine training set and counterfeit training set separately, which we denote as E_z and E'_z, respectively. We set thresholds of z as

$$\lambda_0(z) = E_z, \quad \lambda_1(z) = \frac{(E'_z + E_z)}{2}, \lambda_2(z) = E'_z. \quad (18)$$

IV. Experimental Result

In our banknote processing system, one banknote image is processed by a 200-MHz TMS320C6713 DSP. The average processing times are about 270 ms in high resolution (583×68) and 40 ms in low resolution (145×34). There are two steps in our banknote processing system. At first, the banknote is processed in low resolution and compared to only one reference. If the sensed image is misrecognized in the pre-classification, it will be evaluated as the heavily spoiled banknote and thus be rejected reassuringly. Then, the rejected banknotes will be processed again, in which the sensed image is compared with several potential reference images in low resolution, and the

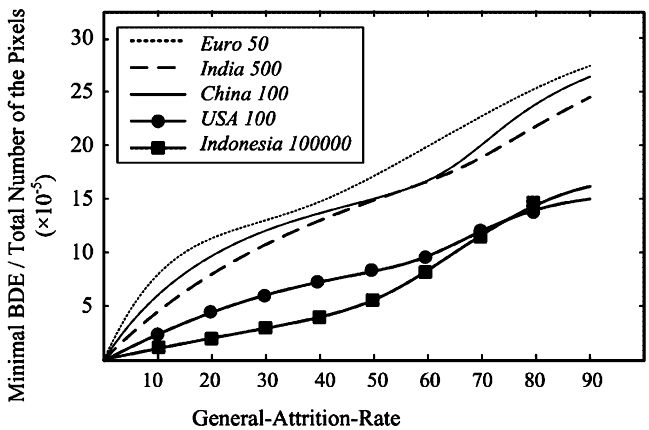

Fig. 3. General attrition rate and BDE.

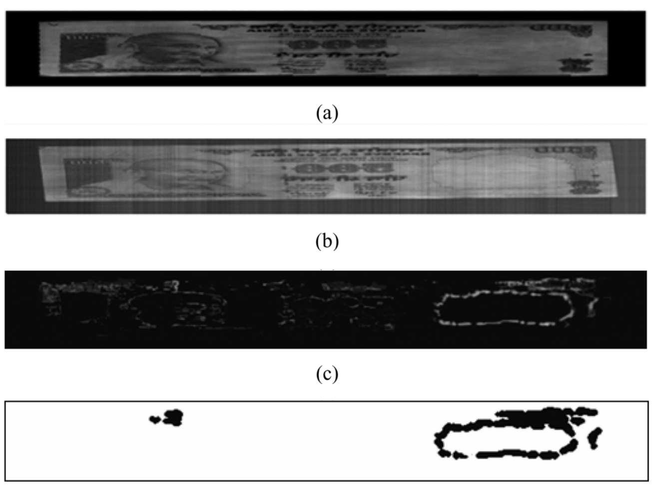

(a)

(b)

(c)

(d)

Fig. 4. Anti-counterfeit feature detection. (a) Genuine banknote image. (b) Sensed counterfeit banknote image. (c) Corresponding BDE map. (d) Anti-counterfeit feature detection result.

reference image with the minimal BDE is selected for the last high-resolution comparison. This two-step strategy leads to high capacity for low-quality banknote processing and greatly decreases the false reject rate.

In our experiment, six kinds of representative banknote are included. Each kind of banknote is manually classified into five grades, and each grade includes 2000 samples. All the banknote images are processed in high resolution. Within each grade, 1000 samples are randomly selected for training, and the rest are used for testing.

Table I demonstrates the correct rates of the general attrition evaluation. We can find that the correct rate of the banknote is correlated to its GAR-BDE curve. As shown in Fig. 3, the GAR-BDE curves of the USA-100 and Indonesia-100000 have smaller slopes than the other curves, and accordingly, their correct rates are relatively low. When a type of banknotes has a basic color similar to μ_w (the expectation of the dust color), it is hard to evaluate their quality by the phenomena of color-shift. The banknotes of the United States follow a serious and sober

TABLE I
CORRECT RATE OF GENERAL ATTRITION EVALUATION (%)

	USA 100	Euro 50	China 100	India 500	Indonesia 100000	Nigeria 1000
uncirculated	92.1	97.4	97.3	96.1	88.9	97.3
ATM satisfied	94.5	98.5	98.7	97.9	90.3	98.0
recyclable	93.6	97.8	98.2	97.6	89.2	97.6
unrecyclable	91.8	97.2	98.4	97.4	94.4	97.6
poor	92.5	97.9	97.8	97.9	97.6	97.1

TABLE II
MIS-DETECTION RATE OF LOCAL DEFECT DETECTION (%)

	USA 100	Euro 50	China 100	India 500	Indonesia 100000	Nigeria 1000
tears	23.1	17.6	18.5	18.1	18.9	18.3
stain	4.7	2.7	2.6	2.9	7.3	2.7
graffiti	11.8	7.8	6.9	7.6	5.4	7.2
holes	0.8	0.3	0.2	0.4	0.2	0.4

TABLE III
FALSE DETECTION RATE OF LOCAL DEFECT DETECTION (%)

	USA 100	Euro 50	China 100	India 500	Indonesia 100000	Nigeria 1000
false rate	7.1	4.3	4.6	4.2	3.9	4.5

design, and therefore yield a relative low correct rate comparing to the other colorful banknotes. The banknotes of Indonesia-100000 are made of plastic instead of paper. The lower adhesion of the plastic causes its special deterioration characteristics.

In the local defect detection, the tear, stain, and graffiti defects on the testing images are initially located manually. Those manually located pixels are then compared with the testing results yielded by our defect detection algorithm. The experimental results are shown in Tables II and III. The algorithm yields similar performance on the processing of the banknotes in different conditions. However, the tear detection is still a difficult task that should be improved in further works.

REFERENCES

[1] F. Takeda and S. Omatu, "High speed paper currency recognition by neural networks," *IEEE Trans. Neural Netw.*, vol. 6, no. 1, pp. 73–77, jan. 1995.

[2] F. Kong, J. Ma, and J. Liu, "Paper currency recognition using Gaussian mixture models based on structural risk minimization," in *Proc. 5th Int. Conf. Machine Learning and Cybernetics*, Dalian, China, Aug. 2006, pp. 3213–3217.

[3] Y. Jin, S. Liu, J. Liu, L. Song, and X. Tang, "An edge-based defect detection algorithm for paper currency," *J. Comput. Res. Develop. (Chinese)*, vol. 44, no. 2, pp. 258–264, Feb. 2007.

[4] C. He, M. Girolami, and G. Ross, "Employing optimized combinations of one-class classifiers for automated currency validation," *Pattern Recognit.*, vol. 37, no. 6, pp. 1085–1096, Jun. 2004.

[5] M. Teranishi, T. Matsui, S. Omatu, and T. Kosaka, "Neuro-Classification of fatigued bill based on tensional acoustic signal," in *Proc. IEEE SMCia/05*, Espoo, Finland, Jun. 2005, pp. 173–177.

[6] H. Cheng and Y. Sun, "A hierarchical approach to color image segmentation using homogeneity," *IEEE Trans. Image Process.*, vol. 9, no. 12, pp. 2071–2082, Dec. 2000.

[7] X. Huang, N. Paragios, and D. N. Metaxas, "Shape registration in implicit spaces using information theory and free form deformations," *IEEE Trans. Patten Anal. Mach. Intell.*, vol. 28, no. 12, pp. 1303–1318, Dec. 2006.